

## Mass-spectrometric and optical study of products from laser-ablated PbTe(Ga)\*

V. A. Mikhailov,\* F. N. Putilin, and D. N. Trubnikov

Department of Chemistry, M. V. Lomonosov Moscow State University, Leninskie Gory,  
119899 Moscow, Russian Federation.

Fax: +7 (095) 939 3952

The products of evaporation ( $p = 10^{-7}$  Torr) from the surface of a PbTe(Ga) target ablated by a focused Nd<sup>3+</sup>: YAl-laser ( $\lambda = 1.08 \mu\text{m}$ ,  $\tau = 15 \text{ ns}$ ,  $w = 0.47 \div 4.8 \text{ J cm}^{-2}$ ) have been studied using quadrupole mass spectrometry and optical spectrometry. Neutral Pb, Te, Ga, Te<sub>2</sub>, and PbTe and singly charged ions of Pb, Te, and Ga were detected by mass spectrometry. The lines of Pb<sup>I</sup>, Pb<sup>II</sup>, Te<sup>II</sup>, and Ga<sup>I</sup> were observed in the 340–760 nm region in the emission spectra; the lines of Pb<sup>III</sup> and Te<sup>III</sup> were absent. The time–current dependences of ions passed through a mass-filter for each vapor component at different  $w$  and for the generation of the crater on the target surface were studied. The kinetic energy of the ions was estimated using an ion-optical decelerating lens. The temperature of the laser plasma was estimated from the intensities of the Pb<sup>I</sup> lines.

**Key words:** laser evaporation, mass spectrometry, emission spectra, optical multichannel analyzer, local thermodynamical equilibrium.

Epitaxial growth of complex semiconductor films produced by using laser evaporation onto a substrate is sensitive to the composition and kinetic energy of the particles of the evaporated material. For example, the presence of rapid ions with energies around hundreds of eV in the vapor reduces the temperature of epitaxial growth due to the formation of vacancy-type defects in the substrate and due to annealing of the transistivity film caused by the bombardment of the film surface. However, the same ions can generate defects in the film itself.<sup>1</sup> Determination of the composition of the laser-evaporated products and the kinetic energy of the particles of the different components present in the vapor is a complicated problem, and its solution requires the use of a number of experimental techniques.

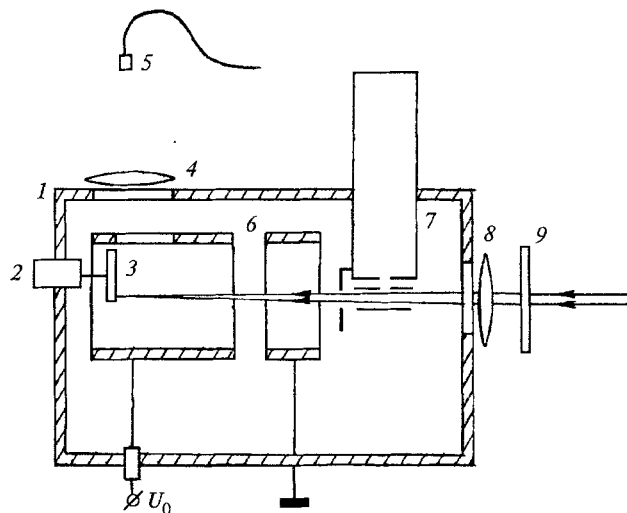
Doped solid solutions based on lead telluride, specifically PbTe(Ga), are interesting objects for the fabrication of thin films. The introduction of gallium into PbTe results in stabilization of the Fermi level nearly in the middle of the forbidden zone. Moreover, long-term distribution processes can be observed at a temperature (80–100 K) typical of PbTe (Ga) resulting in an increase in the photosensitivity of the film and the possibility of accumulating a useful photoconductivity signal.<sup>2</sup>

In this work, a quadrupole mass spectrometer and a multichannel optical spectrum analyzer were applied to determine the composition, kinetic energy, and temperature of particles evaporated from the surface of

PbTe(Ga) at different laser pulse densities  $w$ . The effect of crater or groove generation (on the target surface) on these parameters was also examined.

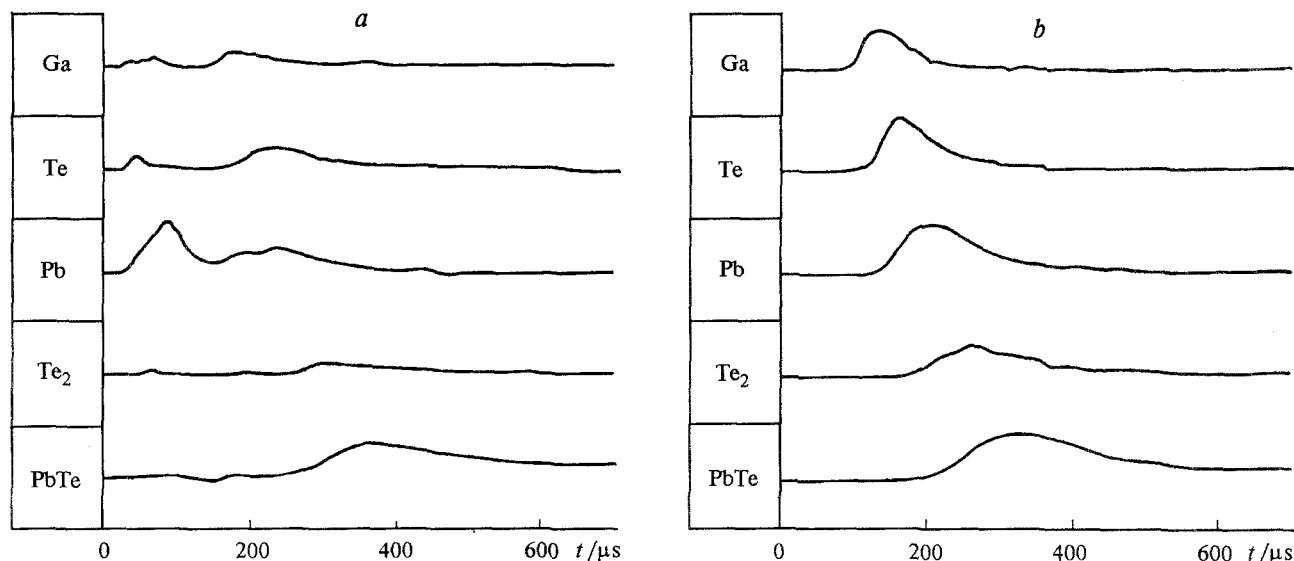
### Experimental

Figure 1 illustrates the scheme of the experiment. To evaporate the particles, a Nd<sup>3+</sup>: yttrium aluminate laser ( $\lambda = 1.08 \mu\text{m}$ ,  $\tau = 15 \text{ ns}$ ,  $w = 0.47 \div 4.8 \text{ J cm}^{-2}$ ) was used. The



**Fig. 1.** A scheme of the experiment: 1, vacuum chamber; 2, target rotation unit; 3, target; 4, collecting lens; 5, lightguide; 6, ion-optical decelerating system; 7, mass spectrometer; 8, focusing lens; 9, optical filters.

\* Submitted as a report at the VI All-Russian Conference on Laser Chemistry, Tuapse, September 18–23, 1993.



**Fig. 2.** Time dependences of the particles of the evaporated substance at  $w = 0.63 \text{ J cm}^{-2}$  (a) and  $w = 3.9 \text{ J cm}^{-2}$  (b). a, only the neutral particles are observed. The gain factor for Te and Pb is 10 times less than for Ga,  $\text{Te}_2$ , and PbTe; b, overall signal for the ions and neutral particles. The gain factor for Ga, Te, and Pb is 10 times less than for  $\text{Te}_2$  and PbTe.

composition of the neutral and charged particles evaporated into a vacuum ( $p = 7 \cdot 10^{-7}$  Torr) was analyzed with a Riber SQ 156 mass spectrometer. The target was placed near the ionization chamber and at a distance of 16 cm from it. In the latter case, the vapor composition was determined both by mass spectra and by emission spectra using an O-SMA optical multichannel spectrum analyzer designed on the basis of a Jobin Yvon HR 640 spectrograph ( $R = 31250$ , dispersion  $12 \text{ Å mm}^{-1}$ ) and a multichannel (1024 channels) detector with an electro-optical convertor. Vapor temperature was determined from the relative intensity of the emission lines of  $\text{Pb}^{\text{I}}$  using a local thermodynamic equilibrium (LTE) approximation.<sup>3</sup>

The time — current dependences of the ions of all components passing through the mass-filter, were evaluated with a Rapid Systems R2000 digital oscillograph with a resolution of 1  $\mu\text{s}$ . Thus, it was possible to investigate the sequence of deposition for each of the components and to estimate the kinetic energies of the particles. For this estimation, an ion-optical system, decelerating and focusing the ions with a fixed energy at the mass spectrometer input, was also used. The advantage of utilizing such a decelerating lens and the principle of operation will be discussed in more detail below.

At the highest chosen values of  $w$ , ions with energies around hundreds of eV were expected to be present in the evaporated material, whereas the voltage amplitude given to the rods of the mass-filter did not exceed 200 V. For this reason, the axis of the mass spectrometer was oriented perpendicularly to the flow of the material. The trajectory of the ions toward the chamber was directed by drawing lenses at the input of the mass spectrometer. With any other geometry of the mass-filter, it would not be possible to separate the ions.

## Results and Discussion

Although the position of the mass-filter was favorably chosen, the mass spectral lines were generally

several times wider than 1 atomic mass unit (amu). Only when a crater formed (at the fixed target) and  $w$  was low, could the isotope composition of the alloy elements be observed. Within the studied range of  $w$ , five major vapor components, Ga, Te, Pb,  $\text{Te}_2$ , and PbTe, were registered in the mass spectrum. Within 340–760 nm, the lines for  $\text{Pb}^{\text{I}}$ ,  $\text{Pb}^{\text{II}}$ ,  $\text{Ga}^{\text{I}}$ , and  $\text{Te}^{\text{II}}$  were also detected. The lines of  $\text{Te}^{\text{I}}$  and  $\text{Ga}^{\text{II}}$  are situated in the farther UV-region and could not be observed under the conditions chosen. The absence of the doubly-charged ions from the mass spectrum agrees with the absence of noticeable  $\text{Pb}^{\text{III}}$  lines at 385.4 and 383.2 nm and the line for  $\text{Te}^{\text{III}}$  at 398.4 nm.

As  $w$  increases, an increase in the intensity of all of the lines in the spectrum is observed. However, the relative intensities and the fraction of neutral and charged particles varied for each component. The time dependences for the flow of the evaporated material also varied with increasing  $w$ . To investigate these variations, the maximum of the corresponding line in the mass spectrum was used for the adjustment of the unit.

Figures 2 and 3 present the time dependences for the evaporated particles passing through the mass-filter. Only neutral particles (Fig. 2, a) were observed at  $w = 0.63 \text{ J cm}^{-2}$ . The intensities of Pb and Te are comparable, while the signal for the mass of Ga is lower than that for the mass of PbTe. The lower the mass of a particle, the faster the particle reaches the detector.

At  $w = 3.9 \text{ J cm}^{-2}$  both neutral and ion particles are generated. Lead is the main component; the intensity of Ga is higher than that of PbTe (Fig. 2, b). The curves of the time dependences for each of the components in the flow contain several peaks, two of which are especially pronounced. The first peak, with respect to exit time,

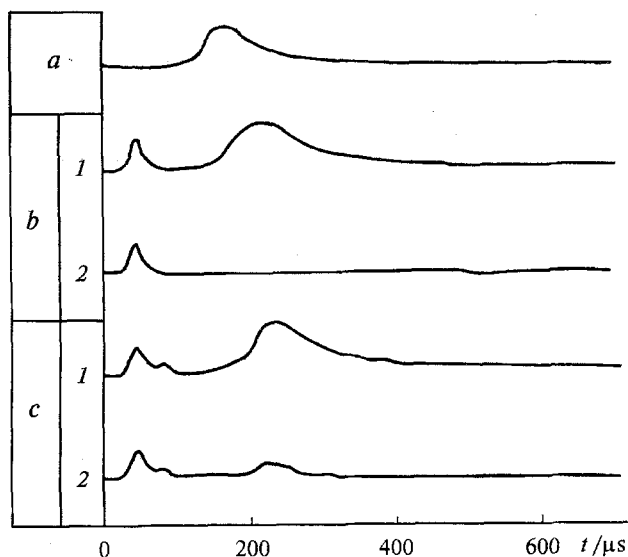


Fig. 3. The time change of the signal for Te mass:  $w = 0.63 \text{ J cm}^{-2}$  (a), only the neutral atoms are observed;  $w = 2.8 \text{ J cm}^{-2}$  (b);  $w = 4.8 \text{ J cm}^{-2}$  (c). 1, overall flow of ions and atoms; 2, ions.

consists of ions while neutral particles were recorded only in the latter peak. Figure 3 presents the change in the behavior of the flow of Te atoms and ions caused by an increase in  $w$ . The ions precede the atoms and form a separate peak. Ions are observed then in the front part of the last peak, which was related initially only to atoms.

$\text{Te}_2$  and  $\text{PbTe}$  were observed mainly as neutral particles. Only at the highest values of  $w$ , was a small amount of the respective ions detected. Within the entire range of  $w$ , the mass line intensities for  $\text{Te}_2$  and  $\text{PbTe}$  were by one or two orders of magnitude lower than those for Te and Pb. The formation of a crater or a groove on the target surface resulted in effects like those caused by reducing  $w$ . For instance, a decrease in the ion portion was observed. The same phenomenon was also recorded in the optical spectra.

Thus, analysis of the time dependences reveals the following features:

- there are definite values of  $w$ , resulting in stable time dependences for the flows of the evaporated particles, specific for each element of the alloy;
- for other values of  $w$ , it can be observed that the nearest stable time dependences vary from pulse to pulse; the nonstability is basically related to the ionic component;
- with an increase in  $w$ , ions appear before neutral atoms, form separate peaks, and then extend to the last peak, initially caused only by neutral particles;
- generation of a crater or a groove results in a change in the time dependences typical of lowering  $w$ .

Direct estimation of the kinetic energy for the particles using the time intervals necessary for the ions to reach the detector is complicated since the time necessary for

the ion to pass through the mass spectrometer tract depends not only on the input potentials, but also on the intrinsic energy of the particles near the input of the mass spectrometer. Thus, the nullifying of the potentials results in the disappearance of the signal at minimal values of  $w$ , when only neutral particles can be recorded. When the target was fixed at a distance of 16 cm from the mass spectrometer input, and the focusing lens was arranged accordingly, the time interval to record the most rapid ions increased. For lead, this increase was  $24 \mu\text{s}$ . The change in the position of the peaks for the corresponding  $w$  varied slightly. This may result from the fact that the separation of the flow of the ions into separate peaks already occurs as the ions pass through the mass spectrometer. The estimation of kinetic energy for the fastest ions based on the changes in the time needed for the ion to appear at the detector is  $48 \text{ eV}$  at  $w = 3.9 \text{ J cm}^{-2}$ . This value is believed to be significantly underestimated for the given  $w$ . Possibly, this energy characterizes the maximum energy level, which can be recorded using a scheme in which the orientation of the mass-filter axis is perpendicular to the flow of particles. The ions with higher energies will not be attracted by the input potentials of the mass spectrometer.

To estimate the kinetic energy of the ions and to avoid the limitations imposed by the instrument at the highest measurement values, we used an ion-optical system, which decelerated and focused the ions with a preselected  $E_0$  at the input of the mass spectrometer. This original lens consists of two coaxial cylinders, one of which is connected with the target and controlled by the voltage  $U_0 = -E_0 e^{-1}$ ; and the other of which is grounded. Calculations indicate that the ions with energies less than  $E_0$  will be reflected by the field located between the cylinders and "destroyed" on the walls of the first cylinder. Ions with energies equal to or slightly exceeding  $E_0$  will be focused at the input of the mass spectrometer, and then decelerated to attain an energy level close to the zero level. From these ions, the mass spectrometer "sorts out" the ions with energies below the instrument limitation. The system, on a whole, functions as an energy filter. By increasing  $|U_0|$  from the zero level, it is possible to record the energy spectrum of the ions including the highest energy  $E_{\text{max}} = |U_{\text{max}}|$  that could be attained under the given conditions of the evaporation, when the signal disappears. Calculations show that with this change in  $|U_0|$ , the time dependences for the flow of ions of the selected mass should be shifted to the beginning of the T-axis, since the faster ions appear earlier despite deceleration.

A similar change was observed experimentally for the time curves at  $w = 2.5 \text{ J cm}^{-2}$  (Fig. 4, a). The signal disappeared at  $U_0 = -2.4 \text{ kV}$ , indicating the absence of Pb ions in the vapor. At higher values of  $w$ , three peaks were recorded in the curves and only the second peak varied in this way (Fig. 4, b). Deviation in the forms of the other two peaks from the behavior expected from the

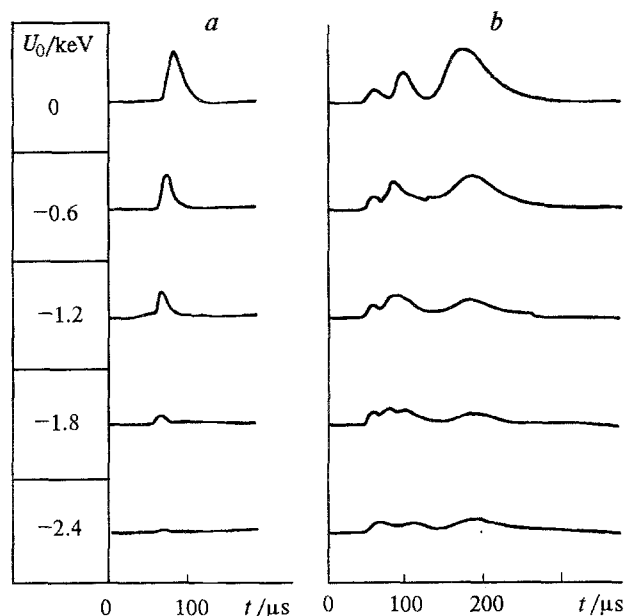


**Fig. 4.** The time dependences of the Pb ion current at different decelerating potentials  $U_0$ : at  $w = 2.5 \text{ J cm}^{-2}$  (a) and  $w = 3.9 \text{ J cm}^{-2}$  (b).

calculations could be related to Coulomb repulsion between the ions and the operational effect of the mass spectrometer. Nevertheless, as in the case of  $w = 2.5 \text{ J cm}^{-2}$ , a decrease in the intensity of the flow passing

through the lens was observed as the decelerating potential increased.

Time dependences of the intensities of the emission lines at a selected distance from the target can also be used to estimate the kinetic energy of the particles.<sup>3</sup> Compared to the mass spectrometric results,<sup>4</sup> this shows that only the fastest particles are registered in the emission spectra.

We were able to evaluate the plasma temperature from the  $\text{Pb}^{\text{I}}$  lines using an LTE-approximation. These estimations are relatively rough since the faster particles have higher temperatures,<sup>3</sup> and the application of LTE to the expanding laser plasma is an equivocal approach. The deviation of the temperature values depends on the choice of the line pairs. However, this estimation, makes it possible to compare the kinetic and heat energies of the flow of the evaporated material. In our case, at  $w = 4.8 \text{ J cm}^{-2}$ , the temperature was  $4500 \div 8000 \text{ K}$  for  $25 \text{ mm}$  in the direction normal to the target.

## References

1. S. V. Gaponov, *Izv. Akad. Nauk SSSR, Ser. Fiz.*, 1982, **46** 1170 [*Bull. Acad. Sci. USSR. Div. Phys. Sci.*, 1982, **46** (Engl. Transl.)].
2. B. A. Akimov, V. P. Zlomanov, L. I. Rjabova, and D. R. Khokhlov, *Vysokochistye veshchestva [High-Purity Substances]* 1991, 22 (in Russian).
3. V. A. Mikhailov, D. N. Trubnikov, R. M. Bodnar, and N. V. Shchedrina, *SFChT*, 1990, **3**, 2777 (in Russian).
4. R. M. Bodnar, V. A. Mikhailov, N. V. Shchedrina, and D. N. Trubnikov, *SFChT*, 1989, **2**, 36 (in Russian).

Received November 5, 1993